## RESEARCH PAPER

# Accurate and efficient study of substrate-integrated waveguide devices using iterative wave method

JAMEL BEN ROMDHAN HAJRI, HAFEDH HRIZI AND NOUREDDINE SBOUI

*This paper proposes an efficient and fast analysis of substrate integrated waveguide (SIW) components using a new approach of the iterative method called WCIP, i.e. "Wave Concept Iterative Process". This method is based on the iterative resolution of waves between two domains. The first is the spectral domain. We use the Floquet–Bloch decomposition to describe all modes in the spectral domain. The second describes the configuration of the circuit in the spatial domain. It allows taking the exact structure according to the appropriate boundary conditions. This method permits to reduce numerical complexity. The convergence of this approach is always guaranteed. The theoretical suggested study is validated by the simulation of two different examples of SIW circuits. The obtained results are in good agreement with those of measurement and with software HFSS simulations, which prove the advantage of this method.*

## I. INTRODUCTION

The substrate-integrated waveguide (SIW) technology combines the advantages of the conventional metallic waveguide and the planar circuit. Thus, they have a high-quality factor, low insertion loss, high integration ability, and low fabrication cost. Hence, it is considered as an important technology to design a high-performance circuit [1–6]. The basic geometry of the SIW circuit consists of a network of metallic cylinders that are embedded in a dielectric substrate layer. These cylinders constitute a lateral discrete metallic as in the case of conventional waveguide.

The analytical study of SIW circuits is solved by empirical formulas of effective physical dimensions [6–8]. All these formulas are restricted in the simple structures and canonical forms such as the waveguide transition. In the case of arbitrary configurations, these expressions are invalid. Hence, the use of a rigorous numerical method is necessary. Several methods are proposed in the literature, which can accurately predict the electromagnetic behavior of SIW devices such as the frequency domain finite differences method, the finite-elements method (FEM) [9, 10], the moments of method [11–13], and semi-analytical method based on the Green Function [12]. The memory usage and the computational time requirements of these methods do not allow the investigation of a wide range of applications which have large size or complex geometry or high number of metallic via-holes.

In this paper, we propose a new approach using the iterative method for a rigorous study of the SIW structures. The iterative method is based on the wave concept [14–16]. The iterative method is already improved for modeling the planar circuits, and it is validated in the multi-layer structures and in periodic problems [14]. This method does not require the treatment of boundary conditions on the truncated computational domains. The relation of field-current is converted to a relation of incidental-reflected waves. The reflexion operator of the waves has an amplitude less than the unit. Therefore, the convergence of this method is guaranteed. The principle of the iterative method is based on the recurrent relation of the transverse incident-reflected waves between the spatial and the spectral domains. The spatial domain is used to satisfy the boundary conditions on the circuit plane. This domain is modeled by a spatial operator, noted $S_\Omega$. The spectral domain is used to calculate the propagation in the medium (air or dielectric). This domain is modeled by a modal operator, noted $\Gamma$. We can better understand the iterative method in [17–19].

The iterative method is adapted to homogenous planar circuit using the transverse waves (at discontinuity interfaces). Therefore, this method is unable to study the SIW devices, which have a network of metallic via-holes embedded in the dielectric layer. In fact, the transverse waves did not permit to take into account the boundary condition of vertical metallic via-hole. In this paper, we develop a new formulation of the iterative method for the analysis SIW circuits, using the concept of the longitudinal waves, which are parallel to the metallic via-holes.

Sciences Faculty of Tunis, University of Tunis El Manar 2092 Tunis, Tunisie
**Corresponding author:**
J. Ben Romdhan Hajri
Email: hajri.jamel83@gmail.com

The basic idea consists in analyzing the SIW circuits as two-dimensional (2D)-periodic structure with defects. In the spectral domain; we assume that the structure is 2D-periodic without defects using the Floquet–Bloch transformation. Therefore, we limit the study to a single cell. Then, in the spatial domain, the boundary conditions, and the continuity equation are satisfied at each cell. The new approach is described in both spectral and spatial domains. We note that in this work we study the case when all metallic via-holes have the same diameter and their height is equal to the thickness of the substrate.

The first section presents the theoretical development of the SIW structures using the modal approach and the Floquet–Bloch Theorem. The second section presents the formulation of the problem using concept of longitudinal waves. We determined the expressions of the electric field and current, and the diffraction matrix $[S]$. In the third part, the computational complexity of the present approach is discussed. Finally, to valid this approach, two different structures are analyzed. The first is a substrate-integrated cavity and the second is a substrate-integrated waveguide quasi-elliptic filter for V-band. Transmission and the reflection coefficients are compared with measurements data and with HFSS software (the FEM method) simulations; then we evaluate the performance of the new method by comparing the error and the computation CPU time with HFSS simulations.

## II. THEORY

The basic schematic of the SIW circuit, presented in Fig. 1 is composed by a dielectric substrate placed between two parallel metal planes (top and bottom), and it contains rows or a network of metallic via-holes.

Considering the planar architecture of the SIW structure, there are two groups of modes: transverse magnetic (TM) with the components ($E_z$, $H_x$, and $H_y$) and transverse electric (TE) with the components ($H_z$, $E_x$, and $E_y$); (where ($E_x$, $E_y$, $E_z$) and ($H_x$, $H_y$, and $H_z$) are, respectively, the components of the electric and magnetic fields). Additionally, the lateral metallic walls (discrete) formed by the metallic via-holes network stop the propagation of modes having the current lines which are perpendicular to the metallic via-holes ($E_x$, $E_y$). Thereafter, only TM modes satisfy the boundary conditions [1, 7], and then the electric fields admit only the one component $E_z$. Consequently, the boundary conditions on the top and bottom metal planes are automatically guarantees and we analyze the boundaries conditions related to the metallic via holes.

## A) Spatial operator

In the propagation medium (dielectric layer), the metallic via-hole is directed along the $z$-direction. We define the
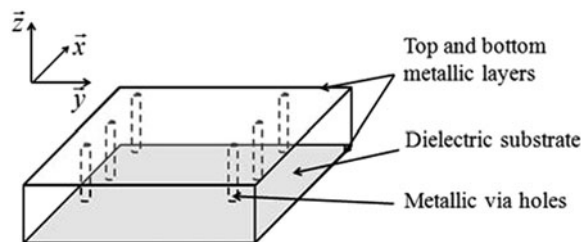


**Fig. 1.** SIW geometry.

incident $A_z$ and reflected $B_z$ waves as a linear combination of electric field $E_z$ and the current density vector $J_z$, (1).

$$\begin{cases} A_z = \frac{1}{2\sqrt{z_0}}(E_z + z_0 J_z), \\ B_z = \frac{1}{2\sqrt{z_0}}(E_z - z_0 J_z), \end{cases} \quad (1)$$

where $z_0$ is the characteristic impedance of the medium.

The discretization process for a SIW cavity example is illustrated in Fig. 2, we distinguish the three sub-domains: sources cells, metallic via-hole cell, and without-metallic-via-hole cell, where $H_\delta$ are their projections matrices, are defined as follows:

$$[H_\delta]_{N_x,N_y} = \begin{cases} 1 & \text{on the sub-domain "}\delta\text{"}; \\ 0 & \text{elsewhere} \end{cases}$$

$$\delta = \begin{cases} s & \text{for the source sub-domain,} \\ v & \text{for the metallic via-hole sub-domain,} \\ nv & \text{for the without-via-hole sub-domain,} \end{cases}$$

where $N_x$ is the number of cells according to the $x$-direction, and $N_y$ is the number of cells according to the $y$-direction.

The boundary conditions for each point of the structure are presented by a spatial coefficient.

The spatial operator $\Omega$ is used to calculate the reflected waves from the incident waves in the spatial domain, as in (2). Its calculation requires the application of the appropriate boundary conditions.

$$A_z(i,j) = [\Omega(i,j)]B_z(i,j) + A_0, \quad (2)$$

where ($i$, $j$) are the coordinates of the cell (in the total structure) according to the $x$-direction and $y$-direction and $A_0$ is the excitation defined on the source domain. The boundary conditions in the all sub-domains are is defined in the
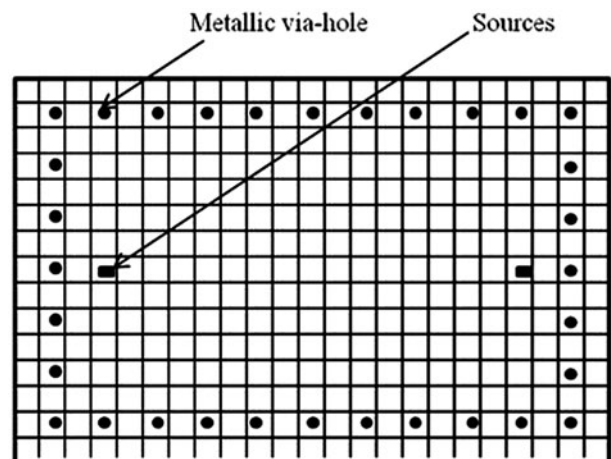


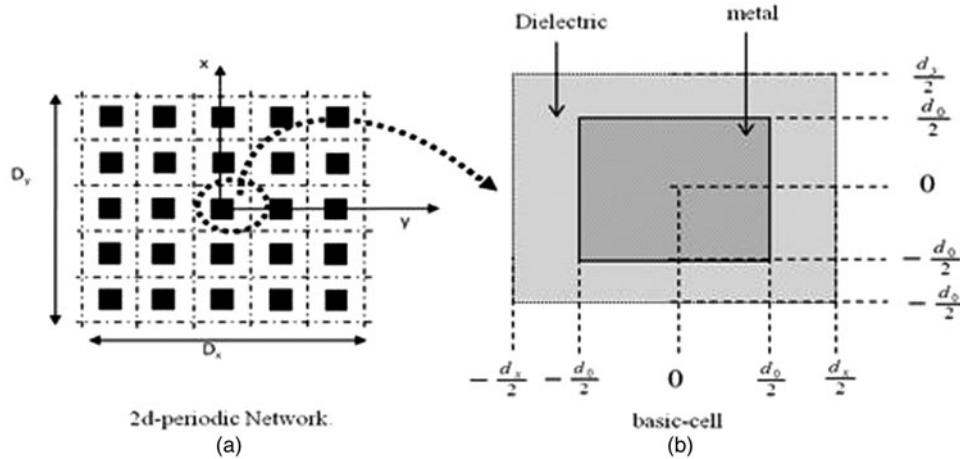**Fig. 2.** Discretization of the spatial domain of a substrate-integrated cavity.

**Fig. 3.** The cross-section of the bi-periodic SIW schema in case of square metallic via-hole (a) and the configuration of the basic cell (b).

following equations (3)

$$
\begin{cases}
\text{On the sub-domain} \quad H_v: \begin{cases} E_z = 0, \\ J_z \neq 0, \end{cases} \\[1em]
\text{On the sub-domain} \quad H_{nv}: \begin{cases} E_z \neq 0, \\ J_z = 0, \end{cases} \\[1em]
\text{On the sub-domain} \quad H_s: \begin{cases} E_z = E_0, \\ J_z = J_0 = \dfrac{E_0}{z_0}, \end{cases}
\end{cases} \tag{3}
$$

where $E_0$ is the excitation source of the circuit.

The use of (1) and (3), allows one to establish the relationship between the incidents and reflected waves, as in (4).

$$
\begin{cases}
H_v \Rightarrow A_z^{k+1} = -B_z^k, \\
H_{nv} \Rightarrow A_z^{k+1} = B_z^k, \\
H_s \Rightarrow A_z^{k+1} = 0 \cdot B_z^{k+1} + A_0,
\end{cases} \tag{4}
$$

where "$k$" is the iteration number.

The general expression for the spatial operator $\Omega$ is given by (5):

$$
\Omega = 0.H_s + H_{nv} - H_v. \tag{5}
$$

## B) Spectral study

The medium is modeled by a spectral operator, which permit to take into account of the scattering behavior. This operator permits to calculate the reflected waves from the incident waves in the spectral domain, as in (6), [14].

$$
[\tilde{B}] = [\Gamma] \cdot [\tilde{A}]. \tag{6}
$$

The connection between the spatial domain and the spectral domain is ensured by a fast transformation in mode using the bi-dimensional fast Fourier transform 2D-FFT and its inverse transform.

$$
\left| \begin{matrix} \tilde{A} \\ \tilde{B} \end{matrix} \right| = FMT \left| \begin{matrix} A \\ B \end{matrix} \right|.
$$

In order to solve the scattering problem, we assume that the structure is 2D-periodic. We consider a bi-periodic array in SIW structure, as depicted in Fig. 3(a). The dimensions of the structure according to $O_x$ and $O_y$ are $D_x$ and $D_y$. The periods according to $O_x$ and $O_y$ are $d_x$ and $d_y$. The effective domain of the metal in the basic cell is $d_0$, as illustrated in Fig. 3(b). The height of the dielectric layer is $h$.

The spectral impedance is obtained from the Helmholtz equation is given by (7), where $\Delta_T$ is the transverse Laplace operator

$$
(\Delta_T + k^2)E_z = j\omega\mu J_z, \tag{7}
$$

where $E$ is the electric field and $J = H \times \vec{n}$ is the current density vector, and $\vec{n}$ is the normal vector.

We consider the modal basis functions given by (8), deduced from the Floquet–Bloch theorem as in [18–20].

$$
\begin{aligned}
\left| f_{pq,mn} \right\rangle &= a_{pq,mn} \cdot \exp\left( j\left( \alpha_p x + \beta_q y \right) \right) \\
&\times \exp\left( j\left( \frac{2\pi m}{d_x} x + \frac{2\pi n}{d_y} y \right) \right) = f_{pq} f_{mn},
\end{aligned} \tag{8}
$$

where $\alpha_p = 2\pi p/D_x$, $\beta_q = 2\pi q/D_y$ are the Floquet–Bloch states, and $a_{pq,mn} = \langle f_{pq,mn} | f_{pq,mn} \rangle$ are the amplitude of the mode $f_{pq,mn}$.

The electric field vector and the current density, using the global modal basis functions (Floquet–Bloch states), are given by (9)

$$
E = \sum_{pq} |f_{pq}\rangle \tilde{E}_{pq} \langle f_{pq}| \quad \text{and} \quad J = \sum_{pq} |f_{pq}\rangle \tilde{J}_{pq} \langle f_{pq}|, \tag{9}
$$

The structure is centered at the origin of the coordinate system (the basic cell is located in the center of the structure). So $-N_x/2 \le p \le N_x/2 - 1$ and $-N_y/2 \le q \le N_y/2 - 1$.

We can write the operator $\Delta_T$ in the modal basis $f_{pq,mn}$ as in (7).

$$
\Delta_T f_{pq,mn} = -\left( \alpha_p + \frac{2\pi m}{d_x} \right)^2 - \left( \beta_q + \frac{2\pi n}{d_y} \right)^2. \tag{10}
$$

The current density is equal to zero in the dielectric area. Thus electric field vector and the current density on metal

sub-domain are given by (11):

$$E_{pq} = \langle \tilde{E}_{pq} \mid h_m \rangle; \quad J_{pq} = \langle \tilde{J}_{pq} \mid h_m \rangle, \qquad (11)$$

where $h_m$ is the effective domain of the metal sub-domain in the basic cell, as illustrated by Fig. 3(b), given by:

$$h_m = \begin{cases} 1 & \text{si}(x, y) \in \left[-\dfrac{d_o}{2}, \dfrac{d_o}{2}\right] \times \left[-\dfrac{d_o}{2}, \dfrac{d_o}{2}\right], \\ 0 & \text{elsewhere.} \end{cases}$$

The spectral impedance $z_{pq}$ connects the components $J_{pq}$ and $E_{pq}$ as in (12):

$$E_{pq} = z_{pq} \cdot J_{pq}. \qquad (12)$$

We can write the impedance operator using the modal base $\langle f_{pq} \mid$ as in (13).

$$z = \sum_{p,q} \mid f_{pq}\rangle z_{pq} \langle f_{pq} \mid. \qquad (13)$$

To take into account the configuration of the basic cell we can decompose the impedance operator on the local modal base: $\langle f_{pq} f_{mn} \mid$, as in (14).

$$z_{pq} = \sum_{m,n} \mid f_{pq} f_{mn}\rangle z_{pq,mn} \langle f_{pq} f_{mn} \mid. \qquad (14)$$

Coupling (7–10–12–14); the impedance operator $z_{pq}$ is given by (15).

$$z_{pq} = \sum_{m,n} \langle H_m \mid f_{pq} f_{mn}\rangle j\omega\mu \frac{1}{k^2 - \alpha_{p,m}^2 - \beta_{q,n}^2} \langle f_{pq} f_{mn} \mid H_m\rangle, \quad (15)$$

where $\alpha_{p,m} = \alpha_p + (2\pi m/d_x)$ and $\beta_{q,n} = \beta_q + (2\pi n/d_y)$. The final expression of the spectral impedance is given by (16)

$$z_{pq} = \sum_{mn} j\omega\mu \frac{\left|\langle H_m f_{pq} f_{mn}\rangle\right|^2}{k^2 - \alpha_{p,m}^2 - \beta_{q,n}^2}, \qquad (16)$$

where $H_m = (1/\sqrt{s})h_m$ and $S$ is the cross-section of metallic via-hole

The propagation constant is given by the following expression: $\gamma_{pq} = \sqrt{(k^2 - \alpha_{p,m}^2 - \beta_{q,n}^2)}$ In the case of shorted-circuited structure with a ground plane at a height $h$, the spectral operator $\Gamma_{pq}$ is given by (17).

$$\Gamma_{pq} = \frac{z_o - z_{pq} \coth\left(\gamma_{pq} h\right)}{z_o + z_{pq} \coth\left(\gamma_{pq} h\right)}. \qquad (17)$$

After the convergence value-iteration of the iterative process, the output parameters are extracted. The distribution of the electric field and the current is given by (18).

$$E_z(i, j) = \sqrt{Z_o}\left(A_z(i, j) + B_z(i, j)\right);$$
$$J_z(i, j) = \frac{1}{\sqrt{Z_o}}\left(A_z(i, j) - B_z(i, j)\right). \qquad (18)$$
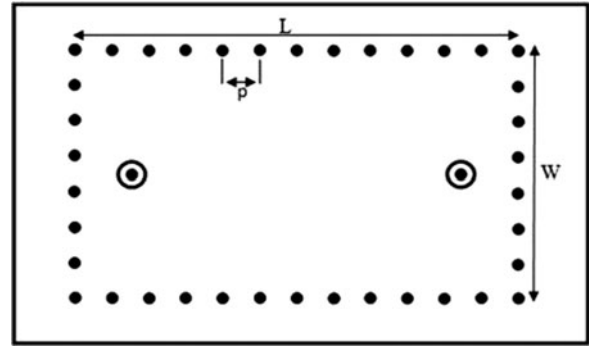


**Fig. 4.** SIW cavity.

The matrix $S$ of the studied structure is given by (19).

$$[S] = \frac{[I_d] - z_o[Y]}{[I_d] - z_o[Y]}, \qquad (19)$$

where $I_d$ is the identity matrix and $Y$ is the admittance matrix of circuit.

## III. APPLICATIONS

The developed approach is used to study tow SIW circuits (for both loss and lossless cases). The first is a substrate-integrated cavity and the second is a quasi-elliptic filter in the V-band.

### A) Integrated substrate cavity

The structure presented in Fig. 4 is a single substrate-integrated cavity first presented in [12], the lateral walls are realized by rows of metallic via-holes. The used substrate is Arlon 25FR (tm) with dielectric constant of 3.58 and thickness of 0.787 mm. The total structure dimensions are $15.17 \times 24$ mm$^2$. The metallic via-holes have the same diameter $d_o = 0.2$ mm and with a period $p = 2$ mm.

To verify the stability of the proposed approach, we have performed a study of the convergence behavior of iterations and of the number of modal bases $(m,n)$. Figure 5 illustrate the convergence curves value- iterations of the reflection and transmission coefficients taken at a frequency equal to 10 GHz. The convergence is reached around 200 iterations (with a ripple rate of $10^{-3}$).
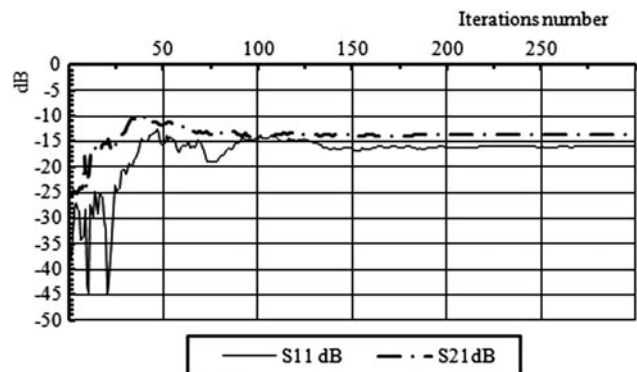


**Fig. 5.** Convergence curves value-iterations of $S$-parameters (Frequency = 10 GHz; Number of iterations = 250 iterations).
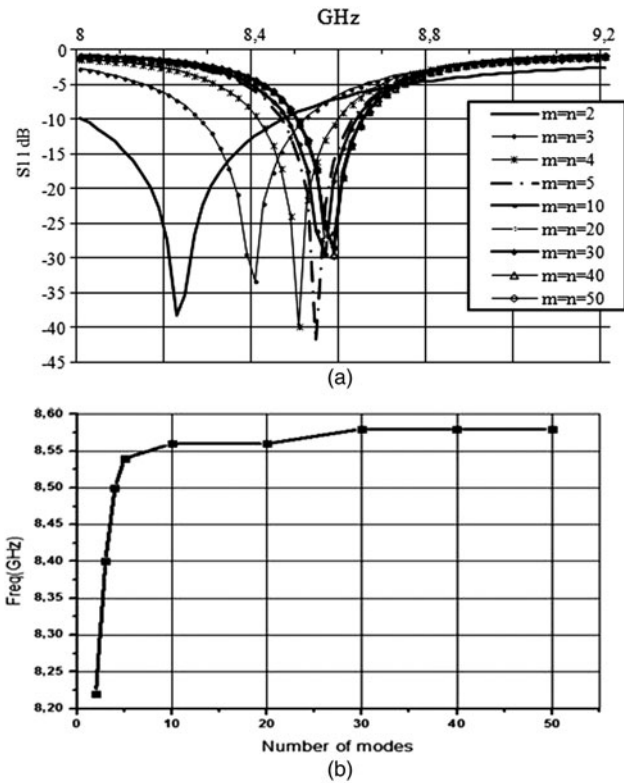
**Fig. 6.** (a) Reflection coefficient for different number of the modes (M,N). (b) Convergence curve of the resonance frequency depending of the number of modes (M,N).
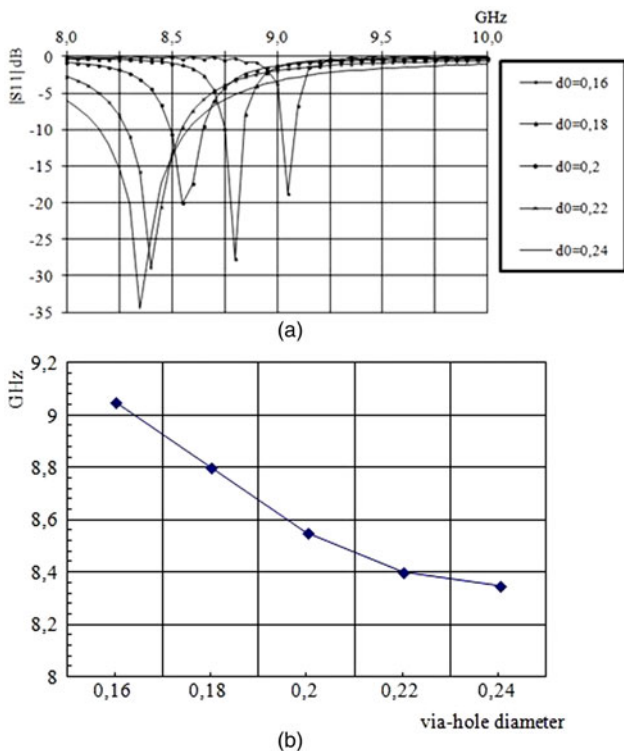
On the other hand, the developed approach is based on the superposition of infinite series of modes. Considering, the limitation of the computational resources which increase considerably with this number, it is necessary to stop this series at a finite number of modes (M,N). In this part, we studied the convergence as function of the number of modes (M,N). The curves in Fig. 6(a) present the reflexion coefficient (S11) for different numbers (M,N).

Figure 6(b) represents the convergence curve of the resonant frequency of the cavity versus (M,N). The convergence value-modes achieved around 30 modes. Therefore, it is unnecessary to take a number of modes higher than 30.

The convergence value-iterations and value-modes show that the proposed method is numerically stable.

Using the same example of the SIW cavity, depicted in the Fig. 4, we study the effect of the diameter of the metallic via-hole on the frequency response. Figure 7(a) depicts the reflection coefficient of different values of the diameter $d_o$. Figure 7(b) presents the behavior of the resonance frequency depending on the diameter of metallic via-hole. The increase of the diameter has effect to decrease the resonance frequency of the cavity.

The results obtained are compared with both measurements that are available in [12] and with data obtained by the FEM (commercial software HFSS). Figures 8(a) and 8(b) display the transmission and reflection coefficients
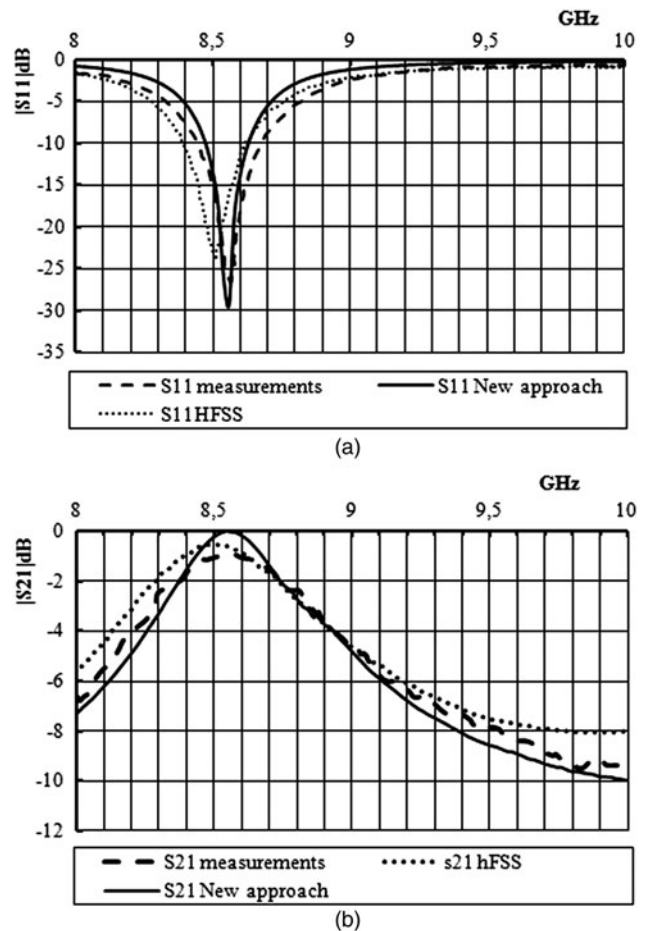


**Fig. 7.** (a) Effect of the diameter of the metallic via-hole. (b) Resonance frequency versus the via-hole diameter.



**Fig. 8.** (a) Reflection coefficient S11 versus frequency. (b) Transmission coefficient S21 versus frequency.

**Table 1.** Computation performance comparison of the proposed method and the FEM method for the SIW cavity example.

|  | Time | Error (%) |
|---|---|---|
| HFSS software | 24 min and 58 s | 6 |
| Our code | 4 min and 47 s | 1.5 |

for the frequency range 8–10 GHz. A satisfactory agreement is observed. This allows validating the accuracy of the present method. Moreover, the HFSS software present a frequency shift of 55 MHz, this shift is close to zero for our method.

All simulations are carried out using a CPU Intel (R) Core (TM) i5 CPU 650@3.20 GHz with a RAM equal to 6 GB. The error and the computation CPU time are recorded in Table 1. The proposed method has the most precise results and the average error does not exceed 2%. Also, the proposed method allows a reduction of the computing time of more than 80%. In fact, the HFSS software becomes very slow if we introduce the metallic via-holes.

## B) Quasi-elliptic V-band filter

The structure showed in Fig. 9 is a quasi-elliptic filter [21]. This circuit is used in high-speed wireless system, in the V-band, with 9 GHz bandwidth. In [22], the multi-mode cavity filter techniques are used to design this circuit. The via-holes have the dimension of $d_0 = 0.25$ mm and spaced of 0.4 mm and the other dimensions of the filter are:

$$b_1 = 2.55 \, \text{mm}, \; b_2 = 1.56 \, \text{mm}, \; b_3 = 6.32 \, \text{mm}, \; b_4 = 1.71 \, \text{mm},$$
$$b_5 = 2.11 \, \text{mm}, \; b_6 = 6.71 \, \text{mm}, \; b_7 = 2.25 \, \text{mm},$$
$$a_1 = 1.84 \, \text{mm}, \; a_2 = 1.84 \, \text{mm}, \; a_3 = 1.65 \, \text{mm}, \; a_4 = 2.5 \, \text{mm},$$
$$a_5 = 1.12 \, \text{mm}, \; \varepsilon_r = 2.1, \; h = 0.2 \, \text{mm}.$$

Figures 10(a) and 10(b) present the reflection and transmission coefficients obtained by both the proposed method and by the commercial software HFSS, and compared with the measurement data available in [21]. A satisfactory agreement is observed.
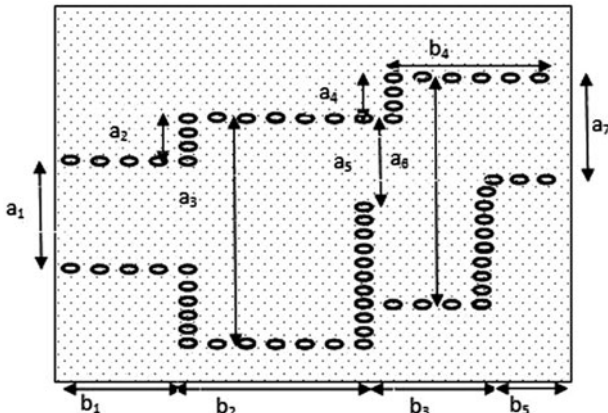


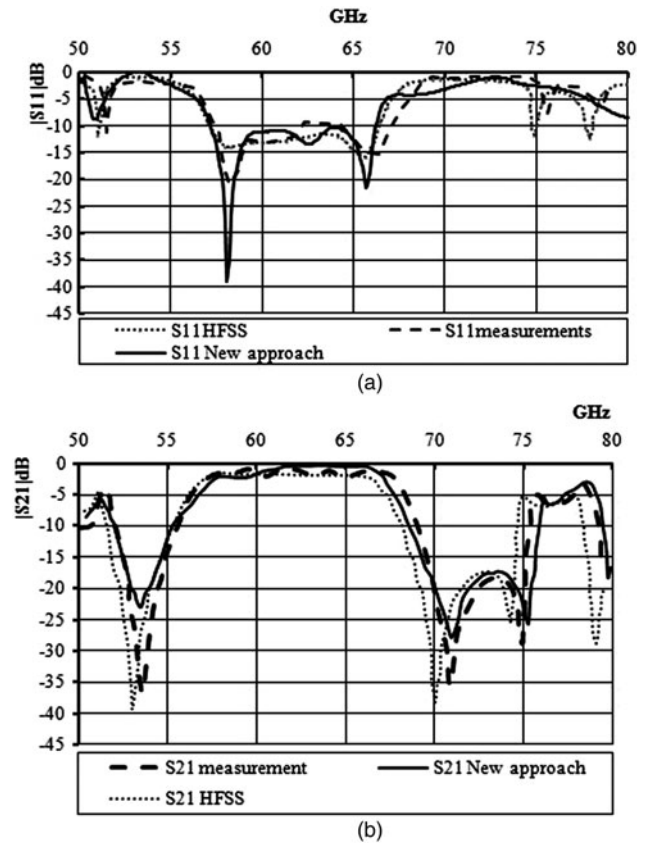**Fig. 9.** Top view of the SIW quasi-elliptic filter.



**Fig. 10.** (a) Reflection coefficient of the SIW quasi-elliptic filter. (b) Transmission coefficient of the SIW quasi-elliptic filter.

## IV. CONCLUSION

This paper presents a new formulation of iterative method used to analyze single-layer SIW circuit. The convergence study allows saving the CPU time and the memory space without sacrificing accuracy. The obtained results are validated by the commercial software HFSS simulations and measurements data available in the literature which prove the accuracy of the method. The proposed method is recommended for the efficient analysis of SIW structures having big sizes.

## ACKNOWLEDGEMENTS

## REFERENCES

[1] Castellano, T. et al.: Feasibility investigation of low cost substrate integrated waveguide (SIW) directional couplers. Progress Electromagn. Res. B, **59** (2014), 31–44.

[2] Bochra, R.; Mohammed, F.; Tao, J.: Analysis of s-band substrate integrated waveguide power divider, circulator and coupler. IJCSIEA, Int. J. Comput. Sci. Eng. Appl., **4** (2) (2014), 1–14.

[3] Kang, H.; Lim, S.: Electrically small dual-band substrate-integrated-waveguide electrically small dual-band substrate-integrated-waveguide antennas with fixed low-frequency and tunable high-frequency bands. IEICE Electron. Express, 11 (5–8) (2014).

[4] Xu, X.; Bosisioand, R.G.; Wu, K.: A new six-port junction based on substrate integrated waveguide technology. IEEE Trans. Microw. Theory Techn., 53 (7) (2005).

[5] Ranjkesh, N.; Shahabadi, M.: Loss mechanisms in SIW and MSIW. Progress Electromagn. Res. B, 4 (2008), 299–309.

[6] Tseng, C.; Chu, T.: Measurement of frequency-dependent equivalent width of substrate integrated waveguide. IEEE Trans. Microw. Theory Techn., 54 (2006), 1431–1437.

[7] Xu, F.; Wu, K.: Guided-wave and leakage characteristics of substrate integrated waveguide. IEEE Trans. Microw. Theory Techn., 53 (1) (2005).

[8] Deslandes, D.; Wu, K.: Accurate modeling, wave mechanisms, and design considerations of a substrate integrated waveguide. IEEE Trans. Microw. Theory Techn. , 54 (2006), 2516–2526.

[9] Ettorre, M.; Sauleau, R.; Le Coq, L.: Multi-beam multi-layer leaky wave SIW pillbox antenna for millimeter-wave applications. IEEE Trans. Antennas Propag., 59 (4) (2011), 1093–1100.

[10] Ettorre, M.; Neto, A.; Gerini, G.; Maci, S.: Leaky-wave slot array antenna fed by a dual reflector system. IEEE Trans. Antennas Propag., 56 (10) (2008), 3143–3149.

[11] Valerio, G.; Casaletti, M.; Seljan, J.; Ettorre, M.; Sauleau, R.: Optimized analysis of slotted substrate integrated waveguides by a method-of-moments mode-matching hybrid approach, in Conf. on Electromagnetic in advanced Applications, Iceea 2013, Torino, Italy, 2013.

[12] Amendola, G.; Arnieri, E.; Boccia, L.: Analysis of lossy SIW structures based on the parallel plates waveguide Green's function. Progress Electromagn. Res. C, 33 (2012), 157–169.

[13] Arnieri, E.; Amendola, G.: Method of moments analysis of slotted substrate integrated waveguide arrays. IEEE Trans. Antennas Propag., 59 (4) (2011), 1148–1154.

[14] Hrizi, H.; Sboui, N.: Reducing the numerical calculation in the wave iterative method by image processing techniques. Appl. Comput. Electromagn. Soc. J., 27 (6) (2012).

[15] Sboui, N.; Gharsallah, A.; Baudrand, H.; Gharbi, A.: Global modeling of periodic structure in coplanar wave guide. Microw. Opt. Technol. Lett., 43 (2) (2004), 157–160.

[16] Sboui, N.; Gharsallah, A.; Gharbi, A.; Baudrand, H.: Global modeling of microwave active circuits by an efficient iterative procedure. Int. J. RF Microw. Comput.-Aided Eng., 148 (3) (2001), 209–212.

[17] Sboui, N.; Gharsallah, A.; Baudrand, H.; Gharbi, A.: Modélisation Electromagnétique Globale des structures Inhomogènes. OHD2007, Valence, France, 5–8 September 2007.

[18] Hamdi, B.; Aguili, T.; Baudrand, H.: Uni-dimensional planar almost periodic structures analysis to decompose central arbitrary located source in spectral domain. IEEE Antenna Technol. Appl. Electromagn. (Antem), (2012).

[19] Guclu, C.; Campione, S.; Capolino, F.: Array of dipoles near a hyperbolic metamaterial: evanescent-to-propagating Floquet wave transformation. Phys. Rev. b89, 155128 (2014).

[20] Islam, R.; Zedler, M.; Eleftheriades, G.V.: Modal analysis and wave propagation in finite 2dtransmission-line metamaterials. IEEE Trans. Antennas Propag., 59 (5) (2011), 1562–1570.

[21] Zelenchuk, D.; Fusco, V.: Low insertion loss substrate integrated waveguide quasi-elliptic filters for v-band wireless personal area network applications. IET Microw. Antennas Propag., 5 (8) (2011), 921–927.

[22] Guglielmi, M.; Jarry, P.; Kerherver, E.; Roquebrun, O.; Schmitt, D.: A new family of all-inductive dual-mode filters. IEEE Trans. Microw. Theory Tech., 49 (2001), 1764–1769.

**Ben Romdhan Hajri Jamel** received the Master degrees in Electronic Systems from the Faculté des sciences de Tunis in 2011. Currently, he is working toward his Ph.D. His research interests are the numerical method for electromagnetic modeling.

**Hrizi Hafedh** is a Doctorate of Electronic. Since 2011 he has been with Institut Supérieur d'Informatique et des Techniques de Communication Hammam Sousse. His current research interests include the modeling of microwave circuits.

**Sboui Noureddine** is a Professor of Electrical Engineering. Since 2002 he has been with the Faculté des Sciences de Tunis. His current research interest includes the areas of numerical methods, electromagnetic field problems, and advanced microwave circuits and components.